IOP Publishing
Fast Track Communications
Plasma Sources Science and Technology
Plasma Sources Sci. Technol. **23** (2014) 022002 (6pp)
doi:10.1088/0963-0252/23/2/022002

Fast Track Communication

Time evolution of the electric field in a Hall thruster

J Vaudolon, B Khiar and S Mazouffre

ICARE-CNRS, 1C. Avenue de la Recherche Scientifique, 45071 Orleans Cedex 2, France

E-mail: julien.vaudolon@cnrs-orleans.fr

Received 8 November 2013, revised 10 January 2014
Accepted for publication 30 January 2014
Published 24 February 2014

Abstract

In order to characterize the natural oscillations of the electric field, the time-dependent Xe^+ ion velocity distribution function is measured in the near-field plume of a low power permanent magnet Hall thruster. The distribution functions are obtained by means of a time-resolved laser-induced fluorescence technique based on a photon-counting method, while time coherence is ensured by applying a sinusoidal potential modulation on a floating electrode. The temporal resolution is 100 ns. The electric field profile is composed of two peaks. This peculiar shape is not yet understood. The electric field is shown to oscillate outside the thruster discharge channel. The results do not reveal the propagation of an ionization front.

Keywords: Hall thruster, oscillations, field, plasma

(Some figures may appear in colour only in the online journal)

1. Introduction

In the field of space propulsion, the necessity to perform various missions requires performance, reliability and versatility. Electric propulsion has the benefit of a low propellant consumption owing to a high propellant ejection speed and a broad operating envelope resulting in mass and cost savings compared with chemical propulsion. Plasma propulsion is mostly dedicated to high velocity increment maneuvers. At present, it is mainly devoted to station keeping and orbit topping for communication satellites. In the near future, this technology will be used to realize full orbit transfer and interplanetary journeys. Many electric devices are available such as arcjets, gridded ion thrusters, Hall thrusters to name only a few [1]. A Hall thruster possesses a large thrust-to-power ratio, which makes this device a powerful candidate to propel the next generation of communication satellites. Despite decades of research on Hall thrusters, the physics at play is far from being fully understood, which slows down the development and optimization of advanced architectures. Careful experiments are therefore needed to validate numerical simulation outcomes and to guide engineers.

A Hall thruster is a cross-field discharge in annular configuration that ionizes a gas to generate thrust [2, 3]. Xenon is usually used owing to its low ionization potential and its high atomic mass. A radial magnetic field traps part of the electrons emitted from an external hollow cathode. The low electron conductivity generates an axially directed electric field that accelerates the unmagnetized ions outside the thruster channel. In a Hall thruster, the electric field is at the origin of the so-called Hall current that is responsible for the efficient ionization of the gas. In addition, it accelerates the ions which generates thrust. The electric field is therefore a fundamental quantity of which properties must be carefully examined. It is well known, and it has been reported in numerous studies, that the discharge of a Hall thruster is highly non-stationary. Plasma fluctuations cover a broad range of frequency and they encompass many kinds of physical phenomena [4]. A better knowledge of the plasma instabilities is necessary in order to improve the performance and the lifetime of these thrusters as they play a major role in ionization and transport processes.

The most common way to measure the time evolution of the electric field in a Hall thruster is to use a fast-moving emissive probe and to differentiate the plasma potential to obtain the electric field. However, this technique is intrusive and it strongly disturbs the discharge [5]. Instead, an optical method can be used. Mazouffre and Bourgeois studied the spatio-temporal characteristics of several ion velocity groups

in the plume of a PPS 100-ML Hall thruster using time-resolved laser-induced fluorescence (TR-LIF) on metastable Xe^+ ions [6]. As explained in the paper, there is the necessity to accumulate photons over several oscillation periods. In that case, the temporal coherence was ensured using a fast power switch which periodically switched off the anode current during 10 μs. The time-varying electric field was measured under these conditions, but the time-averaged discharge behavior was strongly modified by the current break. A recent control technique of the discharge oscillations has been successfully used to perform TR-LIF on a Hall thruster under normal operating conditions [7]. Time coherence is reached by applying a potential modulation on a small electrode located near the cathode exhaust. Resonance can be reached by tuning the modulation frequency. This system does not modify the thruster mean behaviour [7] but keeps the phase of the breathing mode constant. It is believed that such a technique could be used on many discharges to perform time-resolved measurements when coherence is required.

In this contribution we focus on the electric field oscillations observed by means of TR-LIF measurements on the Xe^+ ion population. An active system is used to stabilize the discharge and a photon-counting technique is employed to perform time-resolved acquisitions. The LIF technique allows a direct measurement of the ion velocity distribution functions (IVDFs) along the laser beam. The IVDFs are acquired along the channel axis with a 200 μm spatial resolution. Experiments are carried out in the discharge of a 200 W permanent magnets Hall thruster at a constant discharge voltage of 200 V and an anode mass flow rate of 1.0 mg s^{-1} [8]. The channel width h can be easily modified while keeping the mean diameter d unchanged. Three channel widths can be used by installing three sets of ceramic rings, such that the channel cross-section area is either S_0, two times S_0 or three times S_0, wherein $S_0 = \pi h_0 d_0$ corresponds to the value of standard Hall thrusters, such as the SPT100 value [8]. The so-called $2S_0$ geometry is used. The background pressure is kept under 7×10^{-5} mbar N_2 during operation.

2. Experimental arrangement and diagnostic technique

The experimental technique used to obtain these results has been described in a recent paper [7]. In order to access the time-resolved characteristics of the ion dynamics in the discharge, the LIF technique was coupled with a photon-counting method and with an active stabilization of the discharge to ensure time coherence. The laser beam wavelength is accurately measured by means of a calibrated wavemeter whose absolute accuracy is 80 MHz (~60 m s^{-1}). The time resolution is 100 ns. The discharge oscillations in the spectrum low- frequency band are stabilized by applying a potential modulation on a small electrode near the cathode exhaust which warrants the same frequency content at each time [7]. The discharge properties are therefore quasi-periodic and allow reproducible measurement conditions. The counting card acquisition frequency is 10 MHz which is high enough to observe phenomena in the order of tens to hundreds of kHz. The time-dependent IVDFs are reconstructed from 15 ion velocity groups choosen from mean IVDF obtained through time-averaged LIF measurements using a lock-in technique.

3. Results and discussions

3.1. Time-varying IVDFs

The IVDFs are measured along the axis of the discharge channel from −8 to 10 mm, 0 mm being the exit plane. The channel axis is referred to as the z-axis. Figures 1(a) and (b) show a typical IVDF measurement. The ion velocity is plotted against time at two different locations along the channel axis. The colorbar gives the number of fluorescence photons accumulated over the acquisition period. As can be seen in figure 1(b), different velocity groups can be phase shifted relative to one another in a given IVDF. Figures 2(a) and (b) are two power spectra of the most probable ion velocity groups at 3 mm inside the channel and 4 mm outside. These spectra are obtained using the EMD and Hilbert analysis algorithms [9]. Two frequency bands can be distinguished: a low-frequency band at 14 kHz, which corresponds to the breathing mode, and a high-frequency band at 500 kHz.

3.2. Electric field distribution

Most Hall thruster geometries are based on a constant h/d ratio [2, 8], where h is the channel width and d is the channel mean diameter. This ratio is hereafter referred to as the standard ratio and is identical to that of the SPT100 Hall thruster, for instance. It is shown that the electric field profile along the channel axis can depart from a single peak located near the maximum of the radial magnetic field [10, 11]. In the studies reported by Raitses [11] with emissive probes and by Hargus [10] with both LIF and emissive probes, the electric field distribution may consist of one or two maxima located inside and outside the channel depending on the experimental conditions. For the standard h/d ratio, the number of extrema depends on the thruster operating point [10]. At a normal operating point, one electric field maximum is observed for a narrow channel while a wide channel leads to a split of this peak into two smaller ones [6, 11]. While velocity profiles are accurately measured by means of LIF, the computation of the electric field requires the differentiation of the velocity, a procedure which introduces noise. For an emissive probe, induced perturbations may alter the electric field values. Electric field profiles therefore need to be analyzed with caution. A similar double peak profile can be observed in figure 3 where time-resolved IVDFs are time-averaged to compute the mean electric field $\bar{E}$ according to the energy conservation equation. The electric field reads

$$\bar{E} = \frac{m_i \langle \bar{v_z} \rangle}{e} \frac{\mathrm{d}\langle \bar{v_z} \rangle}{\mathrm{d}z}, \qquad (1)$$

where m_i is the ion mass, e is the elementary charge, $\bar{v_z}$ is the ion mean velocity (first order moment of the IVDF) and brackets indicate temporal averaging. The two peaks are separated by a minimum in the electric field profile. This minimum is located at the thruster exit plane, where the

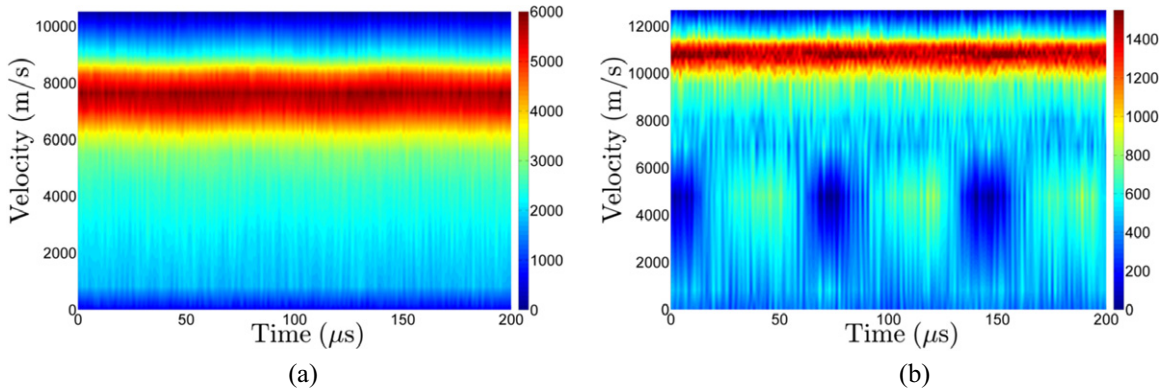

Figure 1. Time evolution of two IVDFs both inside and outside the thruster channel (raw traces): (*a*) IVDF at 3 mm inside the channel; (*b*) IVDF at 4 mm away from the exit plane.

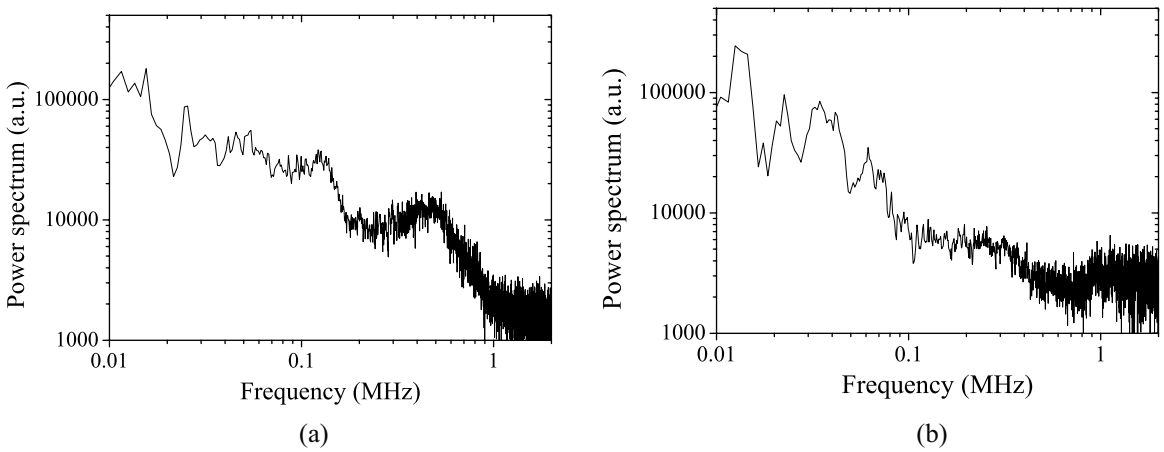

Figure 2. Power spectra of the most probable ion velocity groups: (*a*) spectrum at 3 mm inside the discharge channel; (*b*) spectrum at 4 mm outside the discharge channel of the thruster.

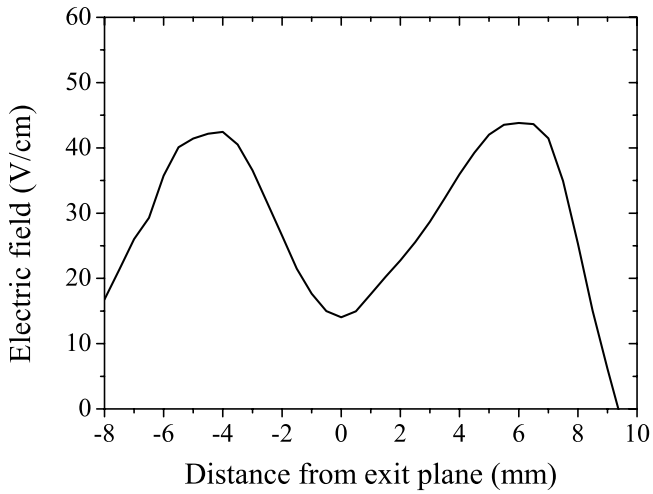

Figure 3. Temporal mean of the axial electric field along the discharge channel.

magnetic field is the highest. The ion density profile assessed from time-averaged LIF spectra is composed of one large peak extending from −6 mm inside the channel to 8 mm outside. Ionization subsequently occurs in a single large area. The electric field is generated by a sharp potential drop due to the high plasma resistivity in the strong magnetic field region. Electron diffusion therefore controls the electric field shape and position. There is no definitive explanation at the present time to account for the electric field distribution. Simulations could prove to be useful to characterize the mechanisms at stake in the present experiments. However, several assumptions can be made to account for the electric field profile. First, the use of a wide channel lowers the plasma/surface interactions. The wall-induced transport characteristics are certainly modified and a new balance is established. It is possible to assume that the plasma/wall interactions control the transport inside the channel while high-frequency microturbulence acts outside. The two mechanisms may also appear together with a varying amplitude along the channel. Note that recent experiments on microturbulence carried out by means of collective Thomson scattering [12] with the PPI thruster show a clear impact of the geometry. The microturbulence level outside the channel is found to decrease when the channel width increases, suggesting that the electron current due to microturbulence decreases, and possibly electron transport [13]. The resulting increase in the plasma resistivity for a wide channel leads to a strong electric field outside the channel, in agreement with our LIF data. This description, however, contradicts the observations of Raitses *et al*, who observed an increase in plasma resistivity inside the channel when the channel was widened. The role of turbulence and wall interactions

on transport is an active topic of research and no definitive conclusions can yet be drawn concerning which mechanism is responsible for the double peak in the electric field. Secondly, the location of the electric field peaks correspond to the region of high magnetic field gradients. The possible effects of the gradient on the electric field distribution generated in such a channel geometry are not reported in the literature. More investigations will be needed to clarify the nature and origin of the double peak in the electric field. Notice that the two-peak structure is not a consequence of the potential modulation on the keeper electrode since this structure has also been observed without driving the cathode.

3.3. Time evolution of the electric field

The time-dependent electric field is computed from the IVDF. An appropriate method consists of using the equation of motion for unmagnetized ions [6]. The ion pressure term can be neglected under the assumption of cold ions. The time-averaged ionization frequency is computed using time-averaged LIF data. The technique described by Perez Luna [14] is used to derive the ionization term, which is found to be one order of magnitude lower than the electric term. The ionization term is therefore neglected. Two-dimensional effects are neglected. Thus, the axial component of the electric field reads

$$E_z = \frac{m_\mathrm{i}}{e}\left(\frac{\partial \bar{v_z}}{\partial t} + \bar{v_z}\frac{\partial \bar{v_z}}{\partial z}\right), \qquad (2)$$

where $\bar{v_z}$ is the ion mean velocity at a given position along the discharge channel axis and at a given time.

Figure 4 shows the time evolution of the accelerating field both inside and outside the channel. The field is plotted as a function of space and time. The z coordinate stands for the distance from the exit plane. The oscillation amplitude inside the channel is weak compared with the oscillation amplitude of the second peak, as illustrated in figure 4. Since the discharge voltage is constant, the outside electric field distribution broadens when diminishing to satisfy

$$U_\mathrm{acc} = \int_\mathrm{channel} E_z(z,t)\,\mathrm{d}z = \text{constant}\ \forall t. \qquad (3)$$

It is verified that $U_\mathrm{acc} = 140\,\mathrm{V}$ at each time. This potential is lower than the applied discharge voltage since one must consider the cathode potential relative to the ground ($-20\,\mathrm{V}$), the cathode and anode sheaths and losses in the system such as radial velocity component and charge-exchange collisions.

The maxima of the electric fields given in the lower and upper plots are separated by $43\,\mu\mathrm{s}$. This delay suggests a wave propagating at $250\,\mathrm{m\,s^{-1}}$, which is close to the velocity of the neutrals. The shift between the peaks is almost π. It is therefore impossible to say whether this front is propagating toward the anode or towards the outside of the thruster. Mazouffre and Bourgeois described the first oscillation cycles after the ignition of the plasma [6]. Their paper describes an electric field front propagating toward the anode at the speed of the neutrals. Assuming the existence of a propagating front, the characteristics observed resemble those described by Mazouffre [6]. However, several experimental differences

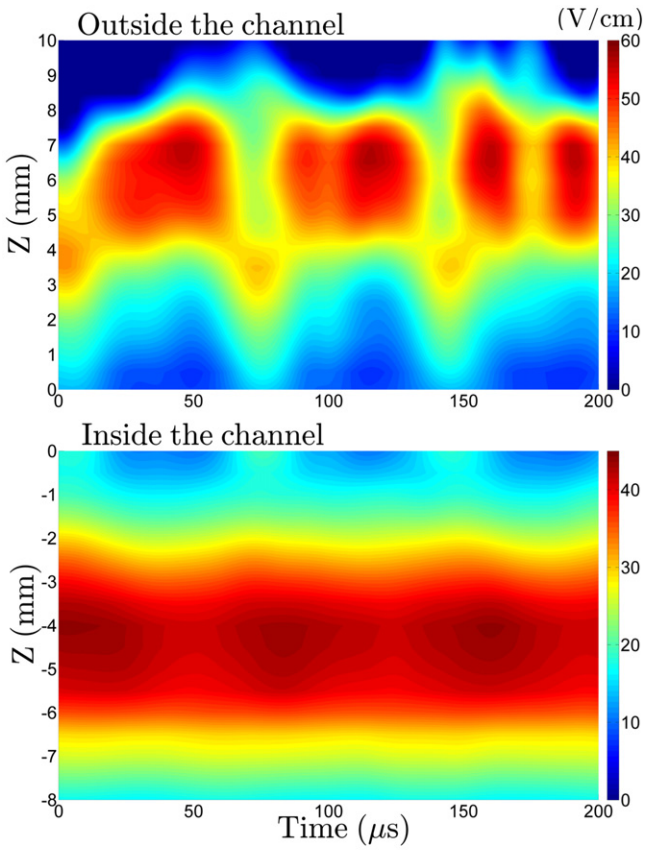

Figure 4. Time evolution of the electric field axial component along the discharge channel. Colorbars are adjusted inside and outside the channel to correctly reveal the oscillations.

exist. Firstly, a geometrical effect is to be considered since a larger h/d ratio is used here instead of the standard ratio. Secondly, the temporal coherence is obtained here through an active modulation of the discharge current that does not modify the thruster mean behaviour [7], while in the study of Mazouffre and Bourgeois, a fast power switch was used to induce strong oscillations [6]. The system used by Mazouffre and Bourgeois has been shown to dramatically change the temporally averaged characteristics of the discharge. The described wave could have been generated by strong discharge current oscillations as the thruster is close to an igniting regime at each cycle. A wave has indeed been shown to propagate during ignition due to a plasma homogeneity in the first breathing oscillation time period [15]. In contrast, the modulation system induces a very low level of oscillation amplitude.

The evolution of the electric field is plotted against the distance from the exit plane in figure 5 for four different instants during a breathing oscillation. The discharge current oscillation is also shown for clarity sake. The internal electric field peak does not move in space and changes slightly in amplitude, while the external one varies from $43\,\mathrm{v\,cm^{-1}}$ at 4 mm to $55\,\mathrm{v\,cm^{-1}}$ at 7 mm downstream of the exit plane.

A characteristic of the breathing oscillations is the back and forth motion of the ionization zone. This leads to a periodic increase in ion density outside the discharge channel.

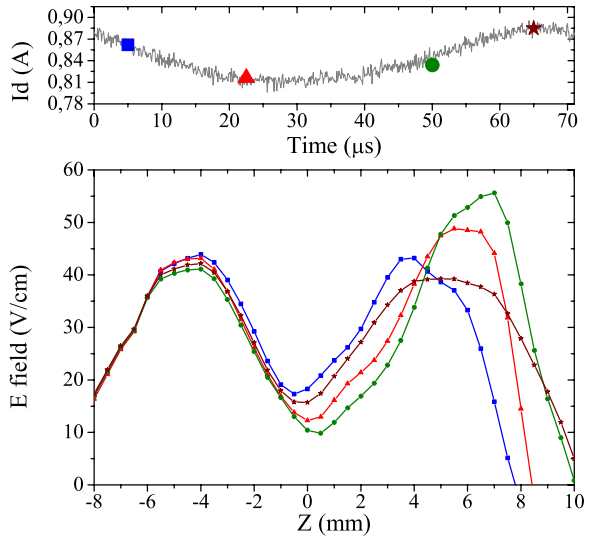

Figure 5. Time evolution of the electric field along the discharge channel at $t = 5\,\mu$s, 22 μs, 50 μs and 65 μs.

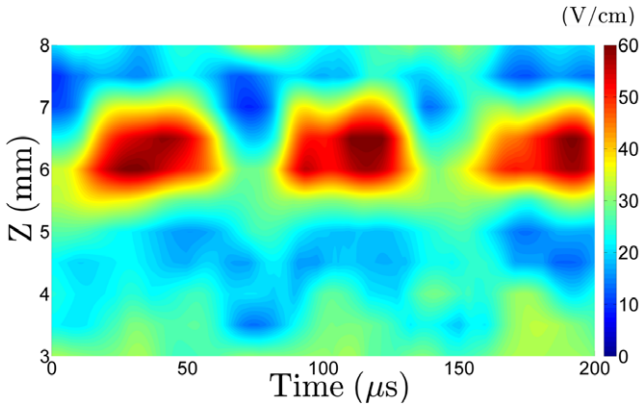

Figure 6. Time evolution of the electric field inferred from the density fluctuations (to be compared with figure 4).

The concomitant electric field can be computed from these variations, assuming that the ground state density profile is similar to the profile of the probed metastable level. Quasi-neutrality can be assumed since the characteristic length of the density gradients is much above the Debye length. We also assume a purely radial magnetic field along the discharge channel axis between $z = 0$ mm and $z = 10$ mm. Collisions are neglected since the various mean free paths are much larger than the characteristic lengths at stake in the measurements. The linearized equation of motion for the magnetized electrons therefore reads

$$m_e \frac{\partial v_{e,z}}{\partial t} = -eE_z - \frac{\nabla p_e}{n} + ev_\theta B_r. \quad (4)$$

The left-hand side term of (4) can be neglected owing to the low electron mass. Thus, the axial electric field is given by

$$E_z = v_\theta B_r - \frac{kT_e}{e}\frac{\nabla n}{n}. \quad (5)$$

The corresponding electric field is shown in figure 6. The electric field computed by this approach is in good agreement with the electric field directly inferred from the measurements with $v_\theta = 400\,\mathrm{km\,s^{-1}}$, $B_r = 0.015\,\mathrm{T}$ and $T_e = 25\,\mathrm{eV}$. B_r and T_e are experimentally measured values while v_θ is a free parameter used to fit the electric field amplitude. The chosen value of v_θ appears to be reasonable since it is on the same order of magnitude as drift velocities typically measured, e.g., in the paper of Frias *et al* [16]. The outside peak of the electric field is therefore attributed to electron density fluctutations generated by the back and forth motion of the ionization zone. The stability of the electric field inside the channel indicates that the ionization zone does not strongly oscillate at the breathing mode in this area. These conclusions are supported by the oscillations of the velocity dispersion which exhibit similar characteristics.

4. Conclusion

Time-resolved measurements of the ion velocity distribution functions along the discharge channel of a Hall thruster are used to determine the time evolution of the electric field in this propulsion device. A photon-counting technique is used to collect the laser-induced fluorescence. The time coherence was ensured using a low power potential modulation on the keeper electrode. Resonance is reached with the plasma parameters by driving the cathode at the breathing mode frequency. The electric field appears to possess two peaks, even though a clarification is still required as to which physical processes would be responsible for such a profile. The results show strong electric field oscillations outside the channel, while internal electric field oscillations are almost absent. The minimum of the electric field is located at the channel exit plane in the region of high magnetic field. The location of this minimum may be attributed to the modification in plasma/wall interactions induced by the use of an enlarged channel compared with the standard geometry.

The electric field oscillations may reveal the propagation of an ionization front at the speed of the neutrals, as in the previous study of Mazouffre [6]. However, in that case, the time coherence was reached by periodically igniting the discharge, which produced strong oscillations as well as strong modifications of the discharge mean behavior compared with a stabilized operating regime. It is believed that such a technique may be at the origin of the wave front observed. The different discharge properties between the two studies may also result from a geometrical effect since a larger channel width is used in this work. The breathing mode phase-locking mechanism induced by the modulation system may also result in discrepancies between the natural and the observed oscillations of the electric field.

Numerical simulations and measurements of the electron properties in the near-field plume are needed to understand the electric field profile and the plasma parameters fluctuations. Furthermore, as can be observed in figure 1, our approach also permits to investigate the oscillations of the electric field in a frequency range between 100 kHz and 1 mHz, a range yet to be explored.

Acknowledgments

The authors greatly appreciated discussions with S Tsikata. J Vaudolon benefits from a CNES-Snecma PhD grant.

References

[1] Jahn R G 2006 *Physics of Electric Propulsion* (New York: Dover)
[2] Dannenmayer K and Mazouffre S 2011 Elementary scaling relations for Hall effect thrusters *J. Propulsion Power* **27** 236
[3] Zhurin V V, Kaufman H R and Robinson R S 1999 Physics of closed drift thrusters *Plasma Sources Sci. Technol.* **8** R1
[4] Choueiri E Y 2001 Plasma oscillations in Hall thrusters *Phys. Plasmas* **8** 1411
[5] Staack D, Raitses Y and Fisch N J 2002 Investigations of probe induced perturbations in a Hall thruster *Proc. 38th AIAA/ASME-/SAE/ASEE JPC (Indianapolis, IN)* paper 2002-4109
[6] Mazouffre S and Bourgeois G 2010 Spatio-temporal characteristics of ion velocity in a Hall thruster discharge *Plasma Sources Sci. Technol.* **19** 9
[7] Vaudolon J, Balika L and Mazouffre S 2013 Photon counting technique applied to time-resolved laser-induced fluorescence measurements on a stabilized discharge *Rev. Sci. Instrum.* **84** 073512
[8] Lejeune A, Dannenmayer K, Bourgeois G, Mazouffre S, Guyot M and Denise S 2012 Ionization and acceleration processes in a small, variable channel width, permanent-magnet Hall thruster *J. Phys. D: Appl. Phys.* **45** 185203
[9] Kurzyna J, Mazouffre S, Lazurenko A, Albarède L, Bonhomme G, Makowski K, Dudeck M and Peradzynski Z 2005 Spectral analysis of Hall-effect thruster plasma oscillations based on the empirical mode decomposition *Phys. Plasmas* **12** 123506
[10] Hargus W A and Cappelli M A 2002 Interior and exterior laser-induced fluorescence and plasma measurements within a Hall thruster *J. Propulsion Power* **18** 159–68
[11] Raitses Y, Staack D, Keidar M and Fisch N J 2005 Electron–wall interaction in Hall thrusters *Phys. Plasmas* **12** 057104
[12] Tsikata S, Lemoine N, Pisarev V and Gresillon D M 2009 Dispersion relations of electron density fluctuations in a Hall thruster plasma, observed by collective light scattering *Phys. Plasmas* **16** 033506
[13] Adam J C, Heron A and Laval G 2004 Study of stationary plasma thrusters using two-dimensional fully kinetic simulations *Phys. Plasmas* **11** 295
[14] Luna J P 2008 Modélisation et diagnostics dün propulseur à effet Hall *PhD Thesis* University of Toulouse
[15] Ellison C L, Raitses Y and Fisch N J 2011 Fast camera imaging of Hall thruster ignition *IEEE Trans. Plasma Sci.* **39** 2950–1
[16] Frias W, Smolyakov A I, Raitses Y and Kaganovich I D 2013 Gradient drift instability in Hall plasma devices IEPC 2013-175 *33rd Int. Electric Propulsion Conf.* (Washington, DC: The George Washington University)